# GSICS SEVIRI-IASI INTER-CALIBRATION UNCERTAINTY EVALUATION

**Tim Hewison**

EUMETSAT, Eumetsat-Allee 1, D-64295 Darmstadt, Germany

**Abstract**

This paper presents an analysis of the uncertainties in the Global Space-based Inter-Calibration System (GSICS) products for the infrared channels of Meteosat/SEVIRI using Metop/IASI as a reference. It is based on the Guide to the Expression of Uncertainty in Measurement (GUM) and aims to provides guidance for users of these GSICS products as well as future evaluations of other products. The inter-calibration algorithm is based on a comparison of collocated observations. This uncertainty analysis allows quantitative trade-offs between the collocation criteria and the number of collocations available, to allow recommendations for further algorithm improvements.

## 1. GENERAL PRINCIPLES

The inter-calibration algorithm is based on the selection of observations from the monitored instrument (Meteosat/SEVIRI) and the reference instrument (Metop/IASI) that are collocated in space, time and viewing geometry. The collocated observations are transformed to be comparable on spatial scales and spectral coverage and compared using a weighted regression. Each collocated observation is allocated a weighting based on its measured spatial variance and the specified radiometric noise of each channel. The regression propagates these variances to estimate the uncertainty on the corrected radiance, which provides a *Quality Indicator* for the inter-calibration product.

In this analysis, uncertainties are analysed through a *measurement model* of the algorithm's processes, as described in the Algorithm Theoretical Basis Document (ATBD) [1]. Each process is considered and the uncertainties evaluated on key variables due to random and systematic effects. These uncertainties are then combined to produce an error budget giving a *Type B* evaluation of the uncertainty on the inter-calibration bias. The random component of this is then compared to the statistics of the standard bias and recommendations made for adjustments of the inter-calibration algorithm to produce more consistent uncertainty estimates. This analysis follows the guidance provided by QA4EO [2], which is based on the Guide to the Expression of Uncertainty in Measurement (GUM) [3].

For each process of the inter-calibration algorithm, typical differences in sampling variables between the monitored and reference instruments are estimated – either from the specified limits used to select the collocations (e.g. spatial sampling), or from the known differences (e.g. in sampling time). These differences are referred to as $\Delta x$ in this document. The sensitivity of the radiances in each collocation to perturbations in each variable is also estimated. This is referred to as $\partial L/\partial x$ in this document.

The quantities input to the inter-calibration process are the radiances, $L$, of each collocation, $i$.
In general, the uncertainty on $L_i$ due to process $j$, is:

$$u_j(L_i) = \Delta x_{i,j}\left(\frac{\partial L}{\partial x}\right)_j , \qquad \textbf{Equation 1}$$

The GSICS Correction, $g(L)$, is based on the regression of collocated radiances observed by the monitored and reference instruments (Section 6.c of the ATBD [1]). It is a function which converts a radiance observed by the monitored instrument, $L$, to be consistent with the calibration of the reference, $\hat{L}$, which is the quantity output from the inter-calibration process:

$$\hat{L} = g(L). \qquad \textbf{Equation 2}$$

In this analysis the observed radiances, $L_i$, are perturbed by $u(L_i)$. Then the regression is recalculated to generate a modified function, $g'(L)$, which will produce different corrected radiances, $\hat{L}'$:

$$\hat{L}' = g'\left(L_i + u\left(L_i\right)\right), \qquad \textbf{Equation 3}$$

This quantifies how errors in the collocated radiances can be propagated through to errors in the GSICS Correction applied to different scene radiances. These provide estimates of the uncertainty on the GSICS Correction, which are converted into brightness temperatures using the derivative of the Planck function evaluated at each scene radiance.

The uncertainties due to various mechanisms introducing systematic and random errors are analysed in the following sections based on case studies. Repeated evaluations with other cases show that the results of the combined uncertainty vary by a factor of ~ ±20%, depending on the distribution of collocated radiances used as input to the calculation of the GSICS Correction. However, this variability is much less than the variability of the evaluation of individual terms, which together limit the accuracy of this uncertainty analysis to a factor of ~2.

## 2. SYSTEMATIC ERRORS

Although the algorithm was designed to ensure samples are symmetrically distributed, in reality small residual differences remain, which may introduce systematic errors in the end products. These sampling differences introduce errors in the radiances of each collocation, depending on their sensitivity to each variable, which is estimated using statistics from case studies. Where information is available on the sampling distribution, this has been used in the analysis – otherwise the collocation criteria have been taken as limits and propagated as standard uncertainties assuming the errors follow rectangular distributions within these limits. These are relatively simplistic treatments and it may be necessary to revise the estimates of one term if it becomes significant and a more accurate analysis is deemed necessary. This follows the approach recommended by ISO 14253-2, which defines an iterative procedure for uncertainty management (*PUMA method*).

### 2.1 Methodology for Systematic Errors

For processes introducing systematic errors, the radiance of each collocated point is perturbed by an amount representing its estimated uncertainty, $u^s_j(L_i)$,

$$u^s_j(L_i) = \Delta x^s_{i,j}\overline{\left(\frac{\partial L}{\partial x}\right)^s_j}, \qquad \textbf{Equation 4}$$

The regression used to calculate the GSICS Correction is recalculated, giving a modified function, $g'(L)$. This function is evaluated for a range of scene radiances and the resulting radiances compared to the corrected radiances generated by the unmodified function, $g(L)$ to provide an estimate of the uncertainty on the corrected radiance due to systematic errors introduced by process $j$:

$$u^s_j\left(\hat{L}\right) = \left|g'_j(L) - g_j(L)\right|, \qquad \textbf{Equation 5}$$

### 2.2 Temporal Mismatch

Systematic differences in the sampling time of the monitored and reference instruments can introduce systematic errors in their collocated radiances due to the diurnal cycle in the temperature, humidity, cloud and, hence, radiance emitted by the Earth's surface and atmosphere.

The selection of orbital data from the monitored and reference instruments are designed to select samples that are distributed with a uniform time difference between the limits specified in the collocation criteria ($\pm\Delta t_{max}$=300 s in this case). For a GSICS Correction derived from $n \approx 30000$ collocations uniformly sampled over a period of $\pm\Delta t_{max}$, it would be expected that the mean time difference would have an uncertainty of $\Delta t = 2\Delta t_{max}/\sqrt{(3n)} \approx 2$ s. However, in practice deficiencies in the

orbital selection cause the mean time difference to be $\Delta t = 30$ s. The sensitivity of the radiances to changes in sampling time has been evaluated by calculating the mean difference between a large ensemble of radiances observed by Meteosat/SEVIRI in successive images.

### 2.3 Longitudinal and Latidinal Mismatches

Systematic errors in the geolocation of both the monitored instrument (SEVIRI) and the reference instrument (IASI) being compared introduce errors in their collocated radiances due to small longitudinal and latitudinal mean gradients in their radiances over the domain of the collocations.

As the exact geolocation error on each pixel is not known, we assume they are distributed uniformly over the accuracies quoted for their navigation. The typical accuracy of the image navigation (rectification) for SEVIRI level 1.5 images based on the operational IMPF processing is calculated to be 1.2 km [4]. The geolocation accuracy of IASI level 1c data is calculated to be 1-2 km [5]. A value of 2 km is taken as a worst case limit – which may be refined later if this term is found to be dominant. These errors are assumed to be partitioned equally between longitude and latitude. Their uncertainties are combined linearly to act as a guard-band, so errors in longitudinal position are assumed to be distributed uniformly over $\pm\Delta lon_{max}=(1.2+2)/\sqrt{2}=2.26$ km. This is equivalent to a standard uncertainty of $\Delta lon=2.26/\sqrt{3}=1.30$ km. The sensitivity of the collocated radiances to systematic errors in longitude was calculated as the mean difference in radiances between adjacent scan *elements* and *lines* of a Meteosat-9 image over the target domain.

### 2.4 Geometric Mismatch

Collocations between different instruments on different satellites are never exactly aligned in terms of viewing and solar geometry. Although the radiances in the infrared channels of SEVIRI-IASI are not sensitive solar and azimuth angles during night-time conditions used in this study, they are affected by the incidence angle – both in terms of absorption along different atmospheric paths and changes in surface emissivity.

Pixels are defined as collocations only if their incidence angles are such that the ratio of their atmospheric path difference is less than 1% (i.e. $|\Delta\sec\theta/\sec\theta|<0.01$). For a typical incidence angle, $\theta = 30°$, this corresponds to a difference $\Delta\theta = 1°$. In practice collocations may have different incidence angles uniformly distributed within the range $\pm\Delta\theta = 1°$. However, if the actual distribution of viewing angles differences is not symmetrically distributed about zero, systematic biases will be introduced into the inter-calibration products. In this case we can use the actual differences in air mass ($\sec\theta$) calculated for the collocations used to calculate a typical GSICS Correction, which follow a rectangular distribution within the limits of $|\Delta\sec\theta/\sec\theta|<0.01$, with a mean value of $\Delta\sec\theta/\sec\theta=-0.00069$.

A radiative transfer model (RTTOV9) was run for a diverse set of 77 atmospheric profiles in three cloud configurations (clear sky, uniform cloud with tops at 700 hPa and 300 hPa) to predict the radiances seen by the infrared channels of SEVIRI. This calculation was repeated at $\theta = 30°$ and $29°$ to estimate the sensitivities, which range from 0.02 K in window channels to 0.11 K at IR9.7.

### 2.5 Spectral Mismatch

When radiances measured with non-identical channels are compared, great care must be taken to account for the differences introduced by their different spectral responses. Many methods have been developed to perform this *spectral correction*. However, no spectral correction method can be perfect and residual errors will remain in the compared radiances, including systematic components. Even using a hyperspectral reference instrument, such as IASI, there are uncertainties introduced in the comparison of collocated radiances with a broadband radiometer, such as SEVIRI, due to hyperspectral instrument's spectral calibration accuracy and gap-filling methods used to account for its incomplete spectral coverage of the GEO channels.

#### *2.5.1 GEO-LEO Spectral Mismatch*

Deficiencies in the hyperspectral LEO reference instrument's coverage of the broadband GEO instrument needs to be accounted for before their collocated observations can be compared. In the case of SEVIRI-IASI inter-calibration a simple approach can be adopted to account for this deficiency

because only SEVIRI's IR3.9 channel has incomplete coverage by IASI, which stops at 2760 $cm^{-1}$. A radiative transfer model (HITRAN) was used to calculate radiance spectra over the full thermal infrared range for nine atmospheres with different cloud amounts. These were convolved with the SEVIRI SRFs and the integral over the full band compared with the integral of those truncated at 2760 $cm^{-1}$. A simple linear model was developed to estimate the radiance over the full SRF from that measured from the truncated SRF. This produced corrections ranging from -0.08 K to -0.35 K depending on the scene radiance. The r.m.s. uncertainty on the linear correction was 0.005 K – but only for the IR3.9 channel.

In general, there will also be contributions from the systematic errors in the radiative transfer model used to perform the spectral correction when comparing the observations of two instruments. However, in the case of SEVIRI-IASI, the uncertainty in the gap filling correction is very small, so the modelling errors will have a negligible influence.

#### *2.5.2 LEO Spectral Calibration Accuracy*

The relative spectral calibration accuracy of IASI is estimated to be $\Delta\nu/\nu=0.5$ ppm [6]. The sensitivity of the collocations' radiances to systematic shifts in the centre frequency of IASI's channels has been estimated by shifting the wavenumbers of the SRFs by this ratio and repeating the spectral convolution. The resulting radiances are negligibly different from those calculated for the unperturbed SEVIRI channels. Even when using a shift of 2 ppm, corresponding to IASI's specified maximum relative spectral calibration accuracy [7], the rms difference in brightness temperature is <1 mK.

#### *2.5.3 GEO Spectral Response Function Interpolation*

The official SRF of SEVIRI's channels is calculated from a series of tests performed on its component parts. These are combined and expressed at irregular wavelength intervals defined to represent the full SRF with minimal errors. However, the SRF definitions are open to interpretation, which may introduce errors in the radiances when compared to a hyperspectral reference instrument. For example, although it is recommended that a linear interpolation is used to convert the published SRFs to the IASI channel wavenumbers, it is possible to use other interpolation methods. The calculations were repeated using linear and quadratic interpolation and the results compared to estimate the magnitude of likely errors introduced due to this ambiguity. This term is quite small (<~0.01 K), and can be neglected if we assume the SRFs are interpreted as recommended and consistently between the application of the GEO observations and in the calculation of the inter-calibration.

### 2.6 Combining and Comparing all Systematic Errors

All the uncertainties due to systematic processes, are added in quadrature to give $u^s(L)$:

$$u^s(L) = \left\{ \sum_j \left( u_j^s(L) \right)^2 \right\}^{1/2}, \qquad \textbf{Equation 6}$$

This total uncertainty on the corrected radiance due to all systematic errors is compared with the contribution from each considered mechanism in Figure 1. Here the uncertainties have been evaluated for the range of radiances observed over all the collocations used in the sample case. The radiances and uncertainties are converted to brightness temperatures for convenient comparison.

Figure 1 shows that generally the systematic mismatches in time and space dominate the total systematic uncertainty due to finite gradients in the scene over the inter-calibration target domain. However, the systematic errors in the IR3.9 channel are dominated by the uncertainty in the spectral correction method applied to compensate for the incomplete coverage of this channel by IASI. Other terms due to geometric mismatches and the spectral calibration of the reference instrument are negligible in all cases and appear erratic due to the limitations of numerical precision.

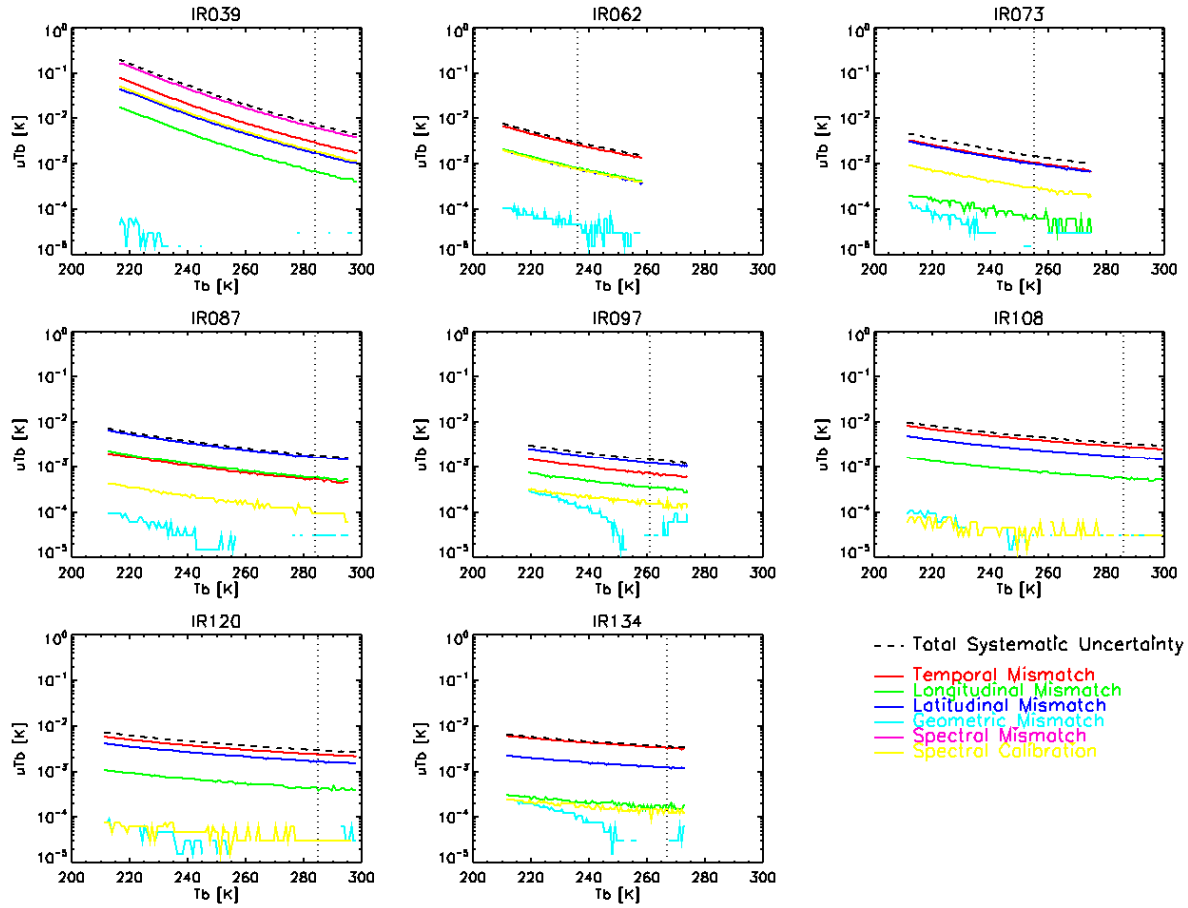


***Figure 1*** **– Contribution of each source of Systematic Error to the Uncertainty of the Brightness Temperatures (Tb) produced by the GSICS Correction for a range of scene radiances for each infrared channel of Meteosat9/SEVIRI using MetopA/IASI reference. Dotted vertical line shows standard scene radiance for each channel.**

## 3. RANDOM ERRORS

Various processes can also introduce random errors on each collocated radiance. The magnitude of these can be estimated from the typical range of each variable and the sensitivity of the radiances to perturbation of each variable, which again can be derived from a statistical analysis of case studies.

### 3.1 Methodology for Random Errors

A Monte-Carlo approach is adopted to evaluate the uncertainty on the final correction for processes which introduce random errors. The radiance of each collocated point is perturbed by an uncertainty calculated by multiplying a random number, $z_i$, drawn from a distribution consistent with a characteristic difference, $\Delta x^r$, multiplied by the sensitivity to random perturbations of this process, $(\partial L/\partial x)^r_j$ as follows:

$$u^r_j(L_i) = \overline{\Delta x^r_j} z_i \overline{\left(\frac{\partial L}{\partial x}\right)^r_j}, \qquad \textbf{Equation 7}$$

The regression used to calculate the GSICS Correction is then re-evaluated with one set of randomly perturbed radiances. The resulting regression coefficients are used to evaluate the bias over a range of scene radiances. This procedure is then repeated a large number ($n_k$) of times to give $n_k$ evaluations of $g'_{j,k}(L)$. Each evaluation of which is used to calculate a corrected radiance for each of a range of scene radiances, $\hat{L}'_{j,k}$.

The standard deviation of $\hat{L}'_{j,k}$ over the Monte Carlo ensemble is then calculated to provide an estimate of the uncertainty on corrected radiances due to each random process, *j*:

$$u_j^r\left(\hat{L}\right) = \left\{ \sum_{k=1}^{n} \frac{\left(g'_{j,k}(L)\right)^2}{n_k\left(n_k - 1\right)} - \sum_{k=1}^{n} \left( \frac{g'_{j,k}(L)}{n_k\left(n_k - 1\right)} \right)^2 \right\}^{1/2}, \qquad \textbf{Equation 8}$$

### 3.2 Temporal Variability

Collocated observations from a pair of satellite instruments are not sampled simultaneously. Variations in the atmosphere and surface during the interval between their observations introduce errors when comparing their collocated radiances. The greater this interval, the larger the contribution of the scene's temporal variability to the total error budget. The uncertainty this introduces to the collocated radiances can be quantified by statistical analysis of a series of SEVIRI scenes described below.

GEO imagers sample scenes at regular intervals: SEVIRI can scan the whole Earth disk every 15 min, or one third of it every 5 min in rapid scan mode. The latter corresponds to the maximum interval recommended in the ATBD for its pixels to be considered collocated with those of IASI. This finite sampling introduces a temporal collocation error with a uniform distribution over $\pm\Delta t_{max} = 300$ s. This is equivalent to an r.m.s. difference between sampling of SEVIRI and IASI observations of $\Delta t = \Delta t_{max} / \sqrt{3} \approx 173$ s. The temporal variability of typical SEVIRI images was originally quantified for each infrared channel in [8]. The root mean squared difference (RMSD) between the channels' radiances was calculated after shifting the images sampled in rapid scanning mode by various intervals.

Here the sensitivity of the radiances to differences in sampling time has been evaluated by calculating the RMSD between a large ensemble of radiances observed by Meteosat/SEVIRI in successive images, after first applying a 5x5 smoothing window, to best reproduce the inter-calibration algorithm.

### 3.3 Longitudinal and Latitudinal Variability

Similarly, collocated observations from a pair of satellite instruments are not exactly collocated and spatial variations in the atmosphere and surface introduce errors when comparing their collocated radiances. The greater the separation between their observations, the larger the contribution of the scene's spatial variability to the total error budget. The uncertainty this introduces to the collocated radiances can be quantified by statistical analysis of a representative SEVIRI scenes described below.

SEVIRI's level 1.5 data has been re-projected onto a grid, with approximately uniform spacing near the sub-satellite point and over the target domain of the collocations, where the median distance between adjacent pixel elements in $\Delta lon_{max} = 3.41$ km and lines in $\Delta lat_{max} = 3.38$ km. It is assumed that the differences in longitude and latitude between collocated radiances measured by SEVIRI and IASI follow uniform distributions over $\pm\Delta lon_{max}$ and $\pm\Delta lat_{max}$.

The spatial variability of a typical SEVIRI image was also quantified for each infrared channel in [8]. The root mean squared difference (RMSD) between the channels' radiances was calculated after shifting the images by various latitude and longitude offsets. As seen in Figure 1 of [8], the RMSD was found to increase approximately linearly with interval for closely separated spatial intervals. Here the sensitivities of the radiances to differences in spatial sampling have been evaluated by calculating the RMSD between all radiances observed by Meteosat/SEVIRI in adjacent pixel elements and lines after first applying the 5x5 smoothing window.

### 3.4 Geometric Variability

Random differences between the viewing and solar geometry of the collocations observed by the monitored and reference instruments also introduce random errors to their collocated radiances. Although the infrared radiances are not sensitive to solar and azimuth angles during night-time conditions used in this study, they are affected by the incidence angle – both in terms of absorption along different atmospheric paths and changes in surface emissivity. As in the case of systematic geometric mismatches (§2.4), the differences in viewing zenith angle between the two sensors is

uniformly distributed within the range $\pm\Delta\theta = 1°$, corresponding to a <1% difference in *air mass*. Likewise, the sensitivity of the collocated radiances to viewing zenith angle is the same as for systematic geometric mismatches.

### 3.5 Spectral Variability

The spectral calibration accuracy of IASI discussed in §2.5 is assumed to also introduce random errors to the collocated radiances, following a normal distribution with $\Delta\nu/\nu$=0.5 ppm and the same sensitivity evaluated in §2.5.

### 3.6 Radiometric Noise

All radiometer observations suffer from radiometric noise caused by limitations of the instruments. This noise contributes to the uncertainty in the comparison of collocated observations. However, the impact of radiometric noise can be reduced by averaging multiple observations, spatially, temporally and spectrally. Furthermore, these terms are implicitly included in both the spatial and temporal variability terms as they are calculated using real observational data, which is subject to radiometric errors. It is, therefore, reassuring to see these terms have negligible contributions to the overall uncertainties. So, although they have been double-counted in the error budget, this does not matter as their contributions are insignificant compared to the temporal and spatial variability of the scene.

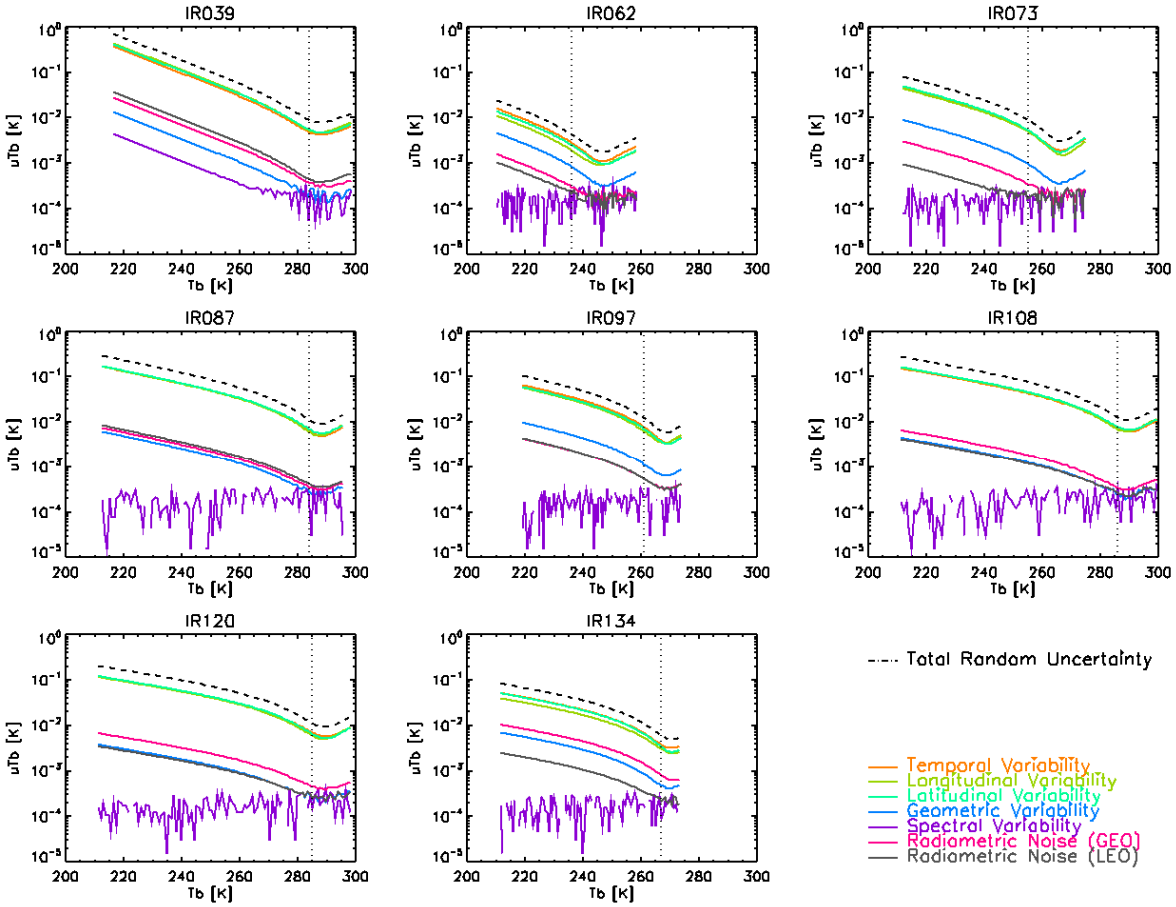


***Figure 2* – Contribution of each source of Random Error to the Uncertainty of the Brightness Temperatures (Tb) produced by the GSICS Correction for a range of scene radiances for each infrared channel of Meteosat9/SEVIRI using MetopA/IASI reference. Dotted vertical line shows standard scene radiance for each channel.**

### 3.7 Combining and Comparing all Random Errors

All the uncertainties due to random processes, are added in quadrature to give $u^r(L)$:

$$u^r(L) = \left\{ \sum_j \left( u_j^r(L) \right)^2 \right\}^{1/2}, \qquad \textbf{Equation 9}$$

This total uncertainty on the corrected radiance due to all random errors is compared with the contribution from each considered mechanism in Figure 2. Here the uncertainties have been evaluated for the range of radiances observed over all the collocations. The radiances and their uncertainties are converted to brightness temperatures for convenient comparison.

Figure 2 shows that the random variability in time and space dominate the total random uncertainty in all channels. Other terms due to geometric and spectral variability are negligible in all cases and the latter appear erratic due to the limitations of numerical precision. These results suggest the time limit of $|\Delta t| < 300$ s specified in the collocation criteria is well matched to the spatial variability due to SEVIRI's 3 km sampling.

## 4. COMBINING SYSTEMATIC AND RANDOM ERRORS

### 4.1 Method for Combining Systematic and Random Errors

The total uncertainties due to systematic and random processes can then be combined to give the total combined uncertainty, $u^c$, for a given radiance, $L$:

$$u^c(L) = \left\{ \left[ u^s(L) \right]^2 + \left[ u^r(L) \right]^2 \right\}^{1/2}. \qquad \textbf{Equation 10}$$

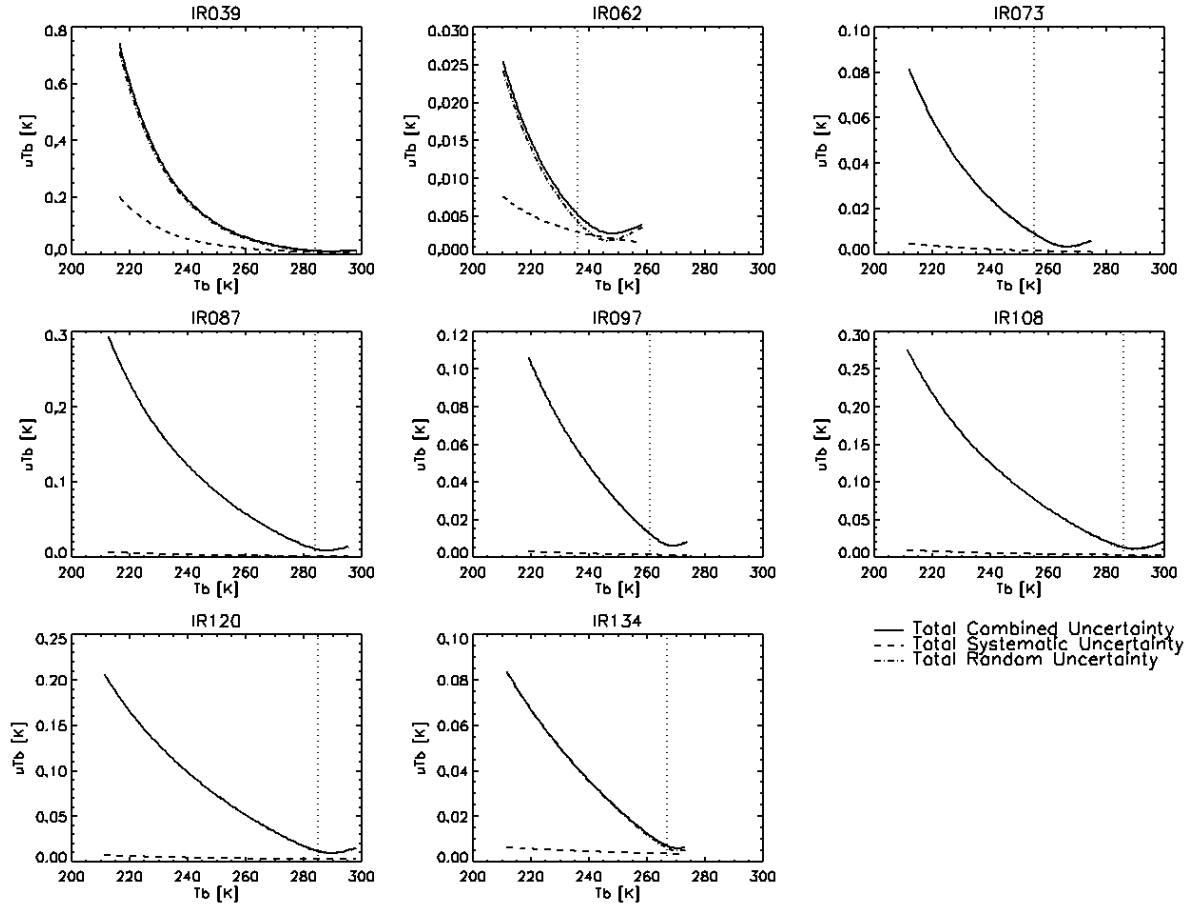


***Figure 3* – Impact of Total Systematic and Random Errors on Uncertainty of the Brightness Temperatures (Tb) produced by the GSICS Correction for a range of scene radiances for each infrared channel of Meteosat9/SEVIRI using MetopA/IASI reference. Dotted vertical line shows standard scene radiance for each channel.**

Figure 3 compares the impact of all the systematic and random errors on the uncertainty of the GSICS Correction evaluated over a range of radiances. This shows that in most conditions the random components of the uncertainty dominate for all channels. It also shows that the uncertainties increase rapidly for low radiance scenes, and reach a minimum near the standard radiances for each channel. This is because the majority of the collocations give radiances near these values, whereas cold, high clouds are relatively infrequent. It is also clear that the uncertainties are much smaller in channels with stronger atmospheric absorption, as the scenes are inherently less variable.

### 4.2 Validation of Quoted Uncertainty on GSICS Correction and Theory

Table 1 compares the total uncertainty due to random errors predicted by this analysis with the median value of the uncertainty quoted within the GSICS Re-Analysis products. This shows the regression used in the ATBD tends to under-estimate the uncertainties by a factor of 1 – 4.

| Meteosat SEVIRI Channel | IR03.9 | IR06.2 | IR07.3 | IR08.7 | IR09.7 | IR10.8 | IR12.0 | IR13.4 | |
|---|---|---|---|---|---|---|---|---|---|
| Standard Scene Radiance | 284 | 236 | 255 | 284 | 261 | 286 | 285 | 267 | K |
| Typical Standard Correction | 0.071 | -0.130 | 0.204 | -0.002 | -0.048 | 0.002 | 0.095 | -1.136 | K |
| Total Random Uncertainty | 0.009 | 0.004 | 0.009 | 0.011 | 0.012 | 0.013 | 0.011 | 0.006 | K |
| Median Uncertainty Quoted | 0.004 | 0.004 | 0.004 | 0.003 | 0.006 | 0.003 | 0.004 | 0.006 | K |
| Rolling SD of Standard Bias | 0.013 | 0.016 | 0.017 | 0.022 | 0.022 | 0.020 | 0.016 | 0.021 | K |
| Total Systematic Uncertainty | 0.008 | 0.003 | 0.002 | 0.002 | 0.002 | 0.003 | 0.003 | 0.004 | K |
| Total Combined Uncertainty | 0.012 | 0.005 | 0.009 | 0.012 | 0.012 | 0.013 | 0.012 | 0.007 | K |

***Table 1;*** **Overall Error Budget of GSICS Correction for SEVIRI-IASI and Validation of Random component**

Table 1 also compares the results of this analysis with the day-to-day variability observed in the biases estimated for standard radiance scenes, calculated as the standard deviation over 15 day windows. These show the GSICS Correction gives more variable results than expected by considering only the random processes affecting the inter-calibration process, which suggests real variations in the instruments' calibration are of the same orders of magnitude as the uncertainties evaluated here.

Also shown in Table 1 are the systematic, random and combined uncertainties of the GSICS Re-Analysis Correction for standard radiance scenes. These values are generally small, with total combined uncertainties ~10 mK. This can be compared to typical levels of the correction for each channel, which are generally an order of magnitude larger. This shows that, although the corrections are small, they are statistically significant at the 95% level for all channels except IR8.7 and IR10.8.

## 5. CONCLUSIONS

This analysis has evaluated the uncertainties for the GSICS Re-Analysis Correction of Meteosat/SEVIRI using Metop/IASI as a reference, with Meteosat operating in normal full-disk scan mode. Random errors on the Near Real-Time corrections would be approximately $\sqrt{2}$ larger due to approximately half the number of collocations being used in the regression. Systematic errors would remain unchanged.

Ideally, the ATBD should be revised to account for correlations within the data when estimating the uncertainty on the GSICS Correction, following this analysis. Alternatively, the uncertainty estimated from the weighted regression in the ATBD should be inflated empirically by a factor of ~2 to achieve greater consistency between the statistics of the GSICS Correction and this analysis.

This analysis does not include contributions associated with the interpretation of the SRFs published for the GEO imager, as explained in §2.5.1. If included, this term could dominate the systematic errors of most channels. This highlights the importance of communicating clear guidance in the application of published SRFs. Although some of these recommendations can be generalised to other pairs of GEO-LEO hyperspectral infrared inter-calibrations, the analysis should be repeated for each inter-calibration product. Particular attention should be paid to the analysis of any gap-filling methods used in spectral corrections, which could dominate the uncertainties for other products not using IASI as a reference.

## 6. REFERENCES


1. Tim Hewison, 2010: *ATBD for EUMETSAT's Inter-Calibration of SEVIRI-IASI*, EUM/MET/REP/08/0468.
2. Nigel Fox, 2010: *A guide to expression of uncertainty of measurements*, QA4EO Guideline QA4EO-QAEO-GEN-DQK-006.
3. JCGM 2008: *Evaluation of measurement data – Guide to the expression of uncertainty in measurement*, http://www.bipm.org/en/publications/guides/gum.html
4. EUMETSAT, 2007: *Typical Geometrical Accuracy for MSG-1/2*, EUM/OPS/TEN/07/0313.
5. IASI L1 Cal/Val Team, 2007: *Presentation of the IASI Level 1 Cal/Val Results*, 23/10/2007, EUMETSAT, Darmstadt
6. B. Tournier and Co-Authors, 2007: *IASI on MetOp-A – Radiometric and spectral performances measured during commissioning*. First IASI Conference, Anglet, France, 13-16 November 2007, http://smsc.cnes.fr/IASI.
7. Denis Blumstein, 2008: *MetOp-A IASI Level 1 Cal/Val at IASI TEC*, GSICS Quarterly, Vol. 2, No. 2, 2008.
8. Tim Hewison, 2009: *Quantifying the Impact of Scene Variability on Inter-Calibration*, GSICS Quarterly, Vol. 3, No. 2.